



Intramolecular cyclization of β -nitroso-*o*-quinone methides. A theoretical endoscopy of a potentially useful innate ‘reclusive’ reaction



Demeter Tzeli^a, Petros G. Tsoungas^{b,*}, Ioannis D. Petsalakis^a, Paweł Kozieliwicz^c, Mire Zloh^{d,e}

^aTheoretical and Physical Chemistry Institute, National Hellenic Research Foundation, 48 Vassileos Constantinou Ave., Athens 116 35, Greece

^bDepartment of Biochemistry, Hellenic Pasteur Institute, 127 Vas. Sofias Ave., Athens GR-11521, Greece

^cSchool of Clinical and Experimental Medicine, University of Birmingham, Edgbaston, Birmingham B15 2TT, UK

^dUCL School of Pharmacy, University College London, 29–39 Brunswick Square, London WC1 1AX, UK

^eDepartment of Pharmacy, University of Hertfordshire, College Lane, Hatfield AL10 9AB, UK

ARTICLE INFO

Article history:

Received 10 September 2014

Received in revised form 24 October 2014

Accepted 6 November 2014

Available online 13 November 2014

Keywords:

β -Nitroso-*o*-quinone methides
Intramolecular *o*- and *peri*-cyclization
Innate reclusive reaction
DFT and MP2 calculations

ABSTRACT

Oxidatively generated β -nitroso-*o*-quinone methides undergo an *o*- and/or *peri*-intramolecular cyclization to arene-fused 1,2-oxazoles, 1,2-oxazines or indoles. The reaction, found to be an innate process, has been scrutinized by DFT/B3LYP and MP2 calculations. Due to its rapidity, the process has been termed a ‘reclusive’ one. Competing *o*-(1,5)- and *peri*-(1,6)- or (1,5)-cyclizations advance via successive transition states. Activation barriers are drastically lowered in AcOH, probably through H hopping or tunnelling whereas they are barely reduced in other solvents. Aromaticity indices, such as HOMA, I_A and ABO, have been used to assess the stability of the end-heterocycles and the preponderance of any one of them. Thus, the preferred cyclization mode, that is, the prevalence or exclusive formation of one of the heterocycles, appears to be oxidant-directed rather than determined by the quinone methide geometry. The question of the *peri*-cyclization, being a primary or a secondary process, has been tackled.

© 2014 Elsevier Ltd. All rights reserved.

1. Introduction

o-Quinone Methides (*o*-QM) **1** (Fig. 1) have enjoyed considerable attention in organic and bioorganic synthesis as reactive intermediates. They have been invoked in biological processes, enzyme inhibition, natural product synthesis and polymer synthesis, such as melanin and lignin.^{1–3} Lately, there has been a resurgence of interest in their chemistry^{2–4} and biology.^{5,6} They play a key role in the chemistry of several classes of antibiotics^{7,8} and antitumour drugs.^{9–11} As highly polarized species, they react with electrophiles¹² and nucleophiles.^{13,14} The latter is the most commonly used and it is usually driven by the re-aromatization of the structure. They are also known to act as DNA alkylating or cross-linking agents.¹⁵ DFT calculations have been reported with sulfur, nitrogen and oxygen nucleophiles.¹⁶ Consequently, many efforts have been directed towards understanding their properties and reaction mechanisms¹⁷ while many approaches have been devised to

generate their structure.^{2–4,18,19} **1** cannot be easily isolated, therefore, it is commonly trapped in situ by (Hetero) Diels–Alder reactions, where **1** acts as the (hetero) diene.^{20,21} The reactions are exceptionally facile, compared with their traditional variants, owing to the transition state and product stabilization provided by the extended π -system.²² Early computational studies on the parent structure **1**^{2,3} as well as some recent DFT-based ones,^{23,24} have focused on deciphering its reactivity as a Diels–Alder component or its biological activity as a Michael acceptor, in aqueous media.^{13,25–27}

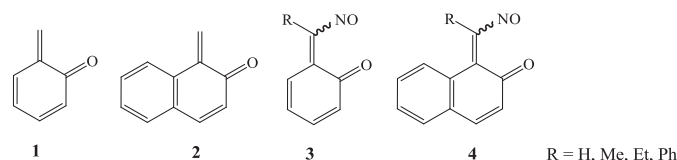
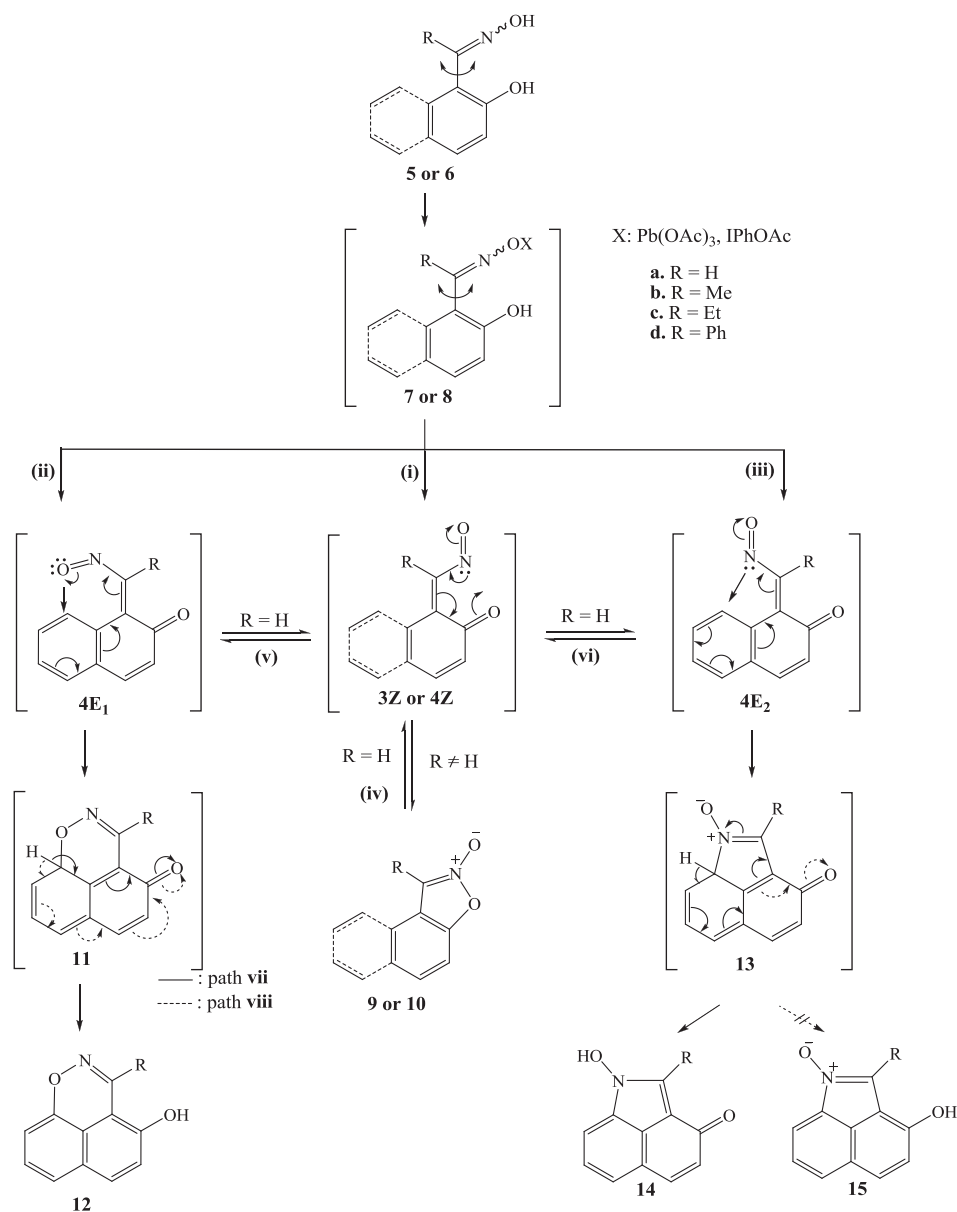


Fig. 1. Structures of *o*-quinone methides **1**, **2** and β -nitroso-*o*-quinone methides **3** and **4** (in the *Z* and *E* conformers, the NO group is towards and away from the carbonyl O atom, respectively. *E* is distinguished as E_1 or E_2 if the nitroso O atom is towards or away from the ring).

* Corresponding author. Tel.: +30 210 6478839; fax: +30 210 6478842; e-mail address: pgt@pasteur.gr (P.G. Tsoungas).

Conjugated β -nitrosoalkenes,^{28–32} a class of reactive molecules, are of significant synthetic potential and are mainly known as 2π or 4π components in cycloaddition reactions. They have been identified by isolation (in some cases, at least),³³ spectroscopic characterization³⁴ or studies of their kinetics and stereo-chemistry.³⁵ In general, they are unstable but their stability increases markedly by halogen, aryl or *t*-alkyl substituents, strong intramolecular H-bonding³⁶ or formation of transition metal complexes.³⁷ These molecules are trapped by reactions similar to those of **1**.^{28–32} A substantial part of their chemistry has been unveiled by Gilchrist^{38,39} and Reissig.^{40,41} The nitrosoalkene motif has been ex-

the structure of **3** and **4** (all its isomers) and the reflection upon their reactivity profile has been recently reported.⁴⁶ Many useful heterocyclic structures have been and can be prepared from these intermediates, fused 1,2-oxazoles **9** or **10** and 1,2-oxazines **12** among them (Scheme 1). 1,2-Oxazoles, C-3 substituted with pharmacophores, is an area of intense research driven by diverse pharmaceutical applications.⁴⁷ The 1,2-oxazole ring, for instance, occupies a prominent position in isoxazole-based marketed drugs, such as, penicillin antibiotics (cloxacillin, dicloxacillin, flucloxacillin), antipsychotics (risperidone, paliperidone), COX 2 inhibitors (parecoxib) to name a few.



Scheme 1. *o*- and *peri*-Cyclization of oxime **5** or **6** *Z/E* isomers, through **7** or **8** and β -nitroso-*o*-quinone methides **3** or **4**.

tensively studied in the *N*-oxide chemistry of furazans⁴² and has also been invoked in the formation of *N*-oxides of 1,2-benzisoxazoles.^{42,43}

β -Nitroso-*o*-quinone methides **3** or **4** (Fig. 1) encompass both **1** and **2** entities. In our earlier reports, they have been proposed as transiently generated during the oxidation of *o*-hydroxyaryl acyloximes.^{42–45} A theoretical insight into the salient features of

It is known that heterocycles with a ring N–O bond are important core structures in many pharmaceuticals. Furthermore, ring opening of these heterocycles, asymmetric reduction in particular, provides access to optically active structures, core components in a variety of medicines.⁴⁸ Indeed, facile ring cleavage of 1,2-oxazine **12**^{43,44} or 1,2-oxazole **9**⁴⁹ lead to chemically and biologically useful outcomes, for instance ring hydroxylation^{43,44} or

diaryl amines as perspective metal ion chelating ligands. It is, thus, the documented significance of **1** (or **2**) and the potential of their nitroso analogues **3** (or **4**) as key intermediates or that of **9** and **12** in (bio)organic synthesis and biology, outlined above, along with some intriguing experimental data,^{44,45} that sparked the present theoretical insight into the pathways of their innate intramolecular reactivity profile.

2. Methodology

The cyclization modes of **3** and **4** were studied in the gas phase and in solution (THF, CH₂Cl₂). AcOH is liberated from the oxidants during the reaction, thus, the latter was studied in the presence of AcOH; AcOH was included in the calculations of stable structures of all minima, intermediates and transition states (see Fig. 2). Minima of intermediates and transition states for tentative pathways were fully optimized using the hybrid B3LYP functional^{50,51} coupled with the 6-311G+(d,p).⁵² However, while the suitability of the B3LYP functional has been questioned, it has, in many cases, been found reliable for theoretical calculations^{53–56} and prediction of organic reaction mechanisms.⁵⁷ Thus, for comparison, additional calculations were carried out for some minima and their intermediate transition states using the aug-cc-pVTZ⁵⁸ basis sets. The credibility of the B3LYP functional was tested using the M06-2X⁵⁹ functional (recommended for the study of non-covalent interactions) (Table 1). The second order Møller–Plesset perturbation theory (MP2) was also used. Relative energies, geometries and harmonic frequencies were also determined for C-3 substituted derivatives (R=H, Me, Et, Ph).

Our calculations show that all three B3LYP, M06-2X and MP2 methodologies give similar geometries. Moreover, they predict similar transition energies and comparable relative energy levels irrespective of the basis set used (Table 1). A larger energy barrier and a more stabilized product was calculated for **4E**₁→**11** reaction (Fig. 4) by the M06-2X functional compared to B3LYP and MP2 techniques; whereas all three techniques gave similar energy barriers and reaction energies for the **17**→**12** reaction (Fig. 4). Clearly, within the same method, both basis sets, 6-311G+(d,p) and aug-cc-pVTZ, give comparable results as do the B3LYP functional with the ab initio MP2 method. It is, thus, safe to consider B3LYP/6-311G+(d,p), as a good choice for our purpose.

For the calculations in THF and CH₂Cl₂ solvents, the polarizable continuum model was employed.⁶⁰ This model is divided into a solute part, lying inside a cavity, surrounded by the solvent part represented as a structureless material characterized by its macroscopic properties, that is, dielectric constants and solvent radius. This method reproduces solvent effects quite well.⁶⁰ For some minima and transition states, their fully optimized geometries in these solvents were found practically identical to those in the gas phase. Hence, single point calculations were carried out at the gas phase geometry for all minima and transition states.

For the calculations with AcOH, the basis set superposition error (BSSE) has been taken into account⁶¹ assuming weak hydrogen bonds among the species formed during the various stages of the reaction.

Harmonic frequencies, performed using the Gaussian 09 program package,⁶² confirmed that the structures are minima or transition states. All calculated minima and transition structures, for R=H, Me, Et and Ph, their absolute energies, relative energies and geometries in the gas phase, in THF and CH₂Cl₂ are given in the Supplementary data section, Fig. 1S. For R=H in the presence of AcOH, the calculated minima and transition structures are given in Fig. 2 and Fig. 2S, where some additional local minima are presented for some structures.

Reformulated HOMA (rHOMA), bond uniformity (*I*_A) and average bond order/bond order deviation (ABO/BOD) have been calculated as aromaticity indices, to assess relative stabilities of the heterocycles. Reformulated HOMA (rHOMA) index^{63–65} has been calculated by the delineated equation.

$$\text{rHOMA} = 1 - \frac{\alpha}{n} \sum_{i=1}^n (R_{\text{opt}} - R_i)^2$$

where *n* is the number of bonds in the aromatic system. *R*_{opt} is the optimum bond length, and *R*_{*i*} is the real bond length of the *i* bond taken into consideration. This equation necessitates the use of the normalization constant α for each type of bond. The used values are $\alpha_{\text{CC}}=257.7$ and $R_{\text{opt}}=1.388$ for CC, $\alpha_{\text{CN}}=93.52$ and $R_{\text{opt}}=1.334$ for CN, $\alpha_{\text{CO}}=157.38$ and $R_{\text{opt}}=1.265$ for CO, $\alpha_{\text{NO}}=57.21$ and $R_{\text{opt}}=1.248$ for NO.⁶⁵

Bond order uniformity index *I*_A^{66,67} and average bond order (ABO) and its deviation (BOD) from ABO index^{68,69} are statistical estimates of bond order variations. *I*_A index is based upon a statistical evaluation of the extent of variation of ring bond order provided by the expression:

$$I_A = 100F(1 - V/V_K), \quad \text{where } V = \frac{100}{N} \sqrt{\frac{\sum (N - \bar{N})^2}{n}}$$

\bar{N} is the arithmetic mean of the *n* various ring bond orders, *N*, is the bond order. *V*_K is the value of *V* for the corresponding non-delocalised form of the ring and *F* is a scaling factor.^{66,67}

3. Results and discussion

Features that dominate a structure invariably accompany or match those that dictate its reactivity. Pertinent to the reactivity of **3** or **4** are the exocyclic β-nitrosoalkene and *o*-quinone methide entities sharing the alkene moiety.

The NO group is a known participant in electrocyclic^{28–30,70} and hetero Diels–Alder cycloadditions.^{28–30,71} In the case at hand it has a multiple engagement. As a substituent it gives rise to *E*- and *Z*-conformers of **3** and **4**. For the *Z* conformer only one minimum is stable. As an ambident nucleophile or electrophile^{72,73} it may trigger intramolecular cyclization to **12** and **14** or **9** and **10** (Scheme 1). Its HOMO is a high energy antibonding combination of N and O lone pairs responsible for its nucleophilicity while orthogonal to those orbitals is a low-lying π* LUMO responsible for its electrophilicity.^{72,73} This feature, as well as its powerful withdrawing ability, accounts for some polarization of the alkene in **3** and **4**. On the other hand, their propensity to aromatize, an inherent substantial driving force, in cooperation with the NO electronic effects, leads to the innate intramolecular cyclization.

Relative energies of *Z*- and *E*-conformers of **3** and **4** have been calculated (Fig. 3 and Table 3S). **3** or **4** for the **a–c** derivatives (Scheme 1) appear to have their lowest energy in the *E*₂ conformation. On the other hand, it is **3d**, in its *Z* conformation, which is of lowest energy. The **3E**₁→**3E**₂ and **4E**₁→**4E**₂ interconversions have very low energy demands of ca. 1.4–4.2 and 0.8–3.1 kcal/mol, respectively (Fig. 3). On the contrary, the **3E**₂→*Z* and **4E**₂→*Z* interconversions have substantial energy barriers of ca. 28.1–34.8 and 18.1–35.2 kcal/mol, respectively.

The energy landscape for the intramolecular *o*- and *peri*-cyclizations of the **3** and **4** minima for R=H is depicted in Figs. 3–6, with or without the AcOH-triggered interactions. That, on the other hand, for the other derivatives is depicted in Figs. 3S–6S. The barriers of all transition states and intermediates are given with respect to **3E**₁ or **4E**₁ conformers, to allow for comparisons between competitive mechanisms.

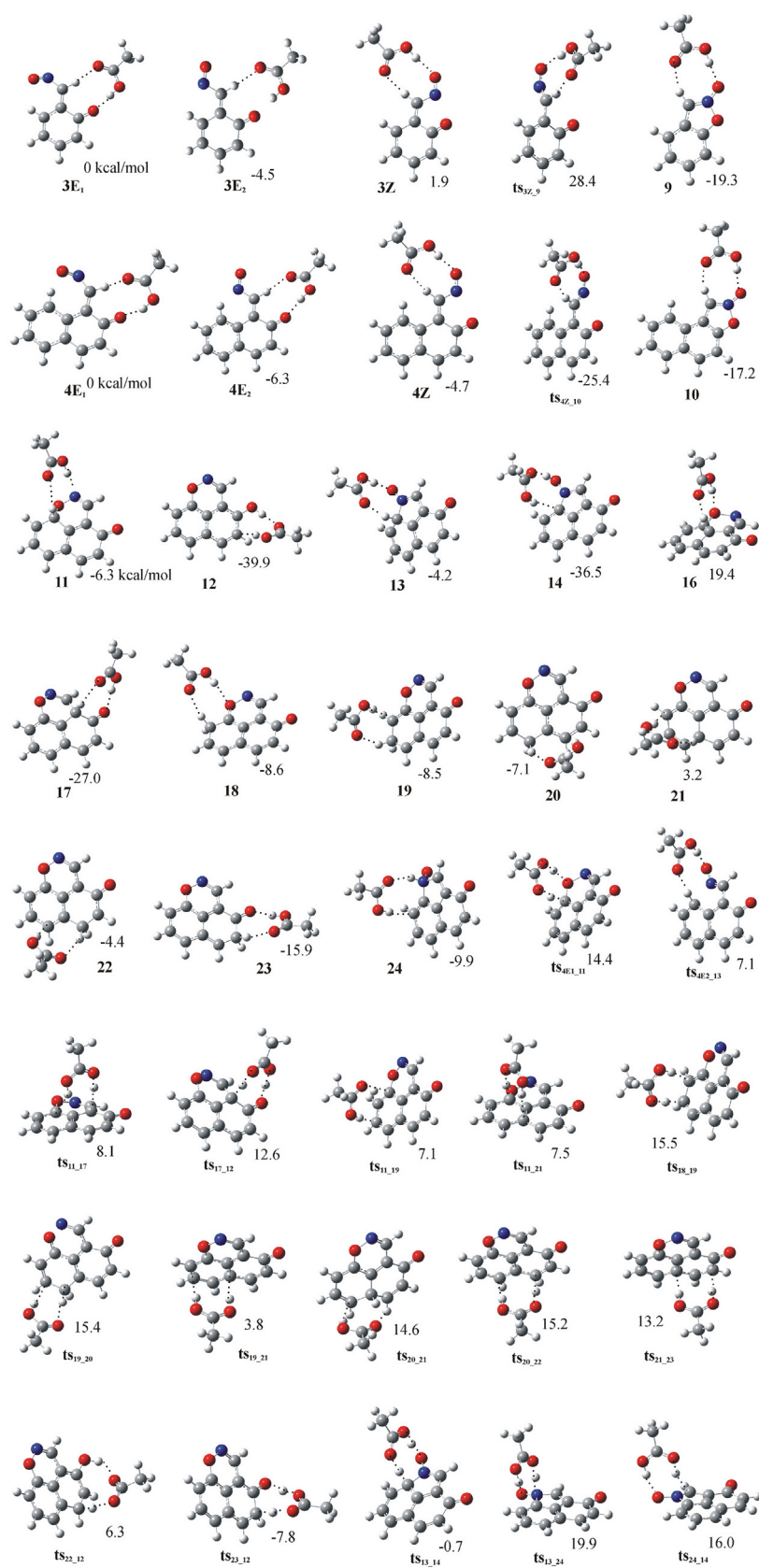


Fig. 2. Minima and transition structures in the *o*- and *peri*-cyclization modes of the β -nitroso-*o*-quinone methides **3** and **4** with AcOH; relative energies in kcal/mol with respect to the 3E₁ and 4E₂ minima structures, respectively.

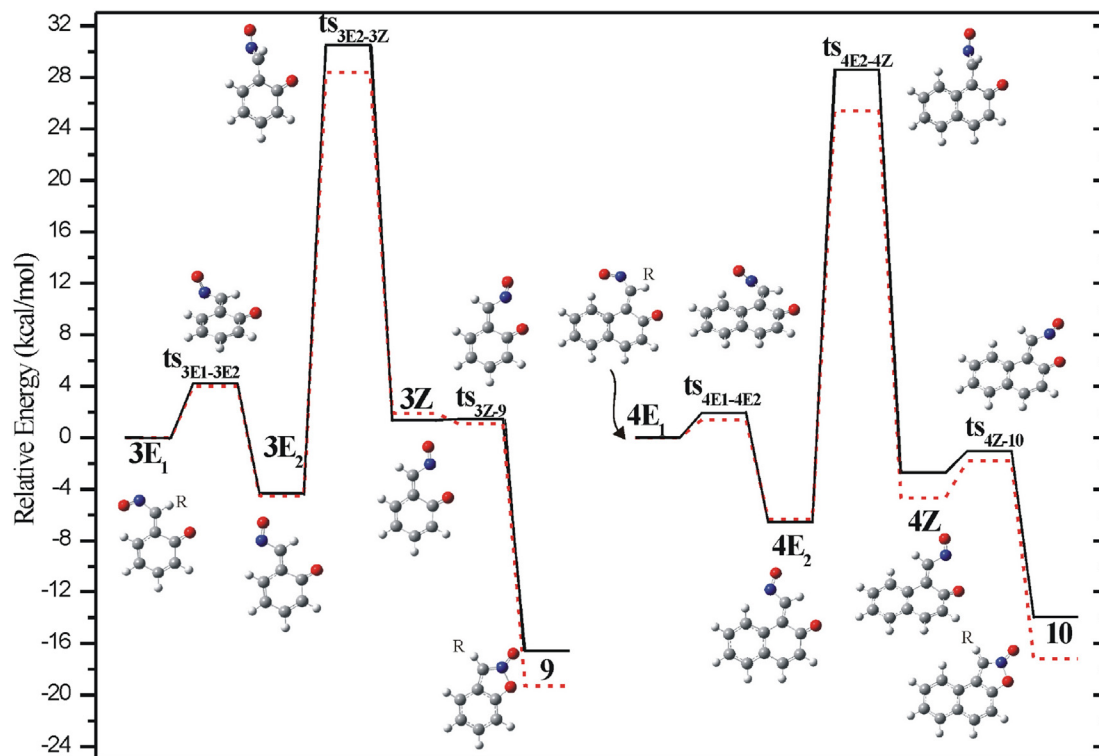


Fig. 3. Relative energies corrected for ZPE of the *o*-(1,5)-cyclization of **3** and **4** minima to **9** and **10** (solid black line) in the presence of AcOH (dashed line) for R=H (C atoms=gray spheres, H=white, O=red and N=blue). Note: C, H and O atoms participating in the cyclizations in this and subsequent figures, are numbered only in a way to facilitate the presentation of results and relevant discussion.

Table 1
Relative energies (kcal/mol) of the calculated minima and transition states included in the $4E_1 \rightarrow 11$ and $17 \rightarrow 12$ reactions calculated at different levels of theory, for R=H^a

	$4E_1 \rightarrow 11$			$17 \rightarrow 12$		
	$4E_1$	ts_{4E_1-11}	11	17	ts_{17-12}	12
B3LYP/6-311+G(d,p)	0	8.3	-4.5	0	56.6	-14.4
B3LYP/aug-cc-pVTZ	0	8.1	-5.2	0	58.1	-16.0
M062X/6-311+G(d,p)	0	13.5	-8.2	0	58.9	-13.9
M062X/aug-cc-pVTZ	0	13.1	-9.0	0	57.2	-15.9
MP2/6-311+G(d,p)	0	7.3	-3.6	0	56.7	-12.9

^a Minima **4**, **11**, **12** and **17** are depicted in Figs. 3 and 4.

3.1. *o*-(1,5)-Cyclization

o-(1,5)-Cyclization, with the NO group acting as an electrophile, takes place through the Z conformer (Scheme 1, path (iv), Fig. 3 and Fig. 3S).

Non zero but very low energy barriers were calculated for **3a** and **4a,b** of 0.1, 1.7 and 0.3 kcal/mol, respectively. An insignificant elevation is observed in solution with the corresponding barriers being 0.5, 3.1 and 0.7 kcal/mol (Fig. 3S). *o*-Cyclization of the other derivatives of **3** and **4** occurs instantaneously as the near zero energy barrier indicates (Scheme 1, path (iv), Fig. 3S). These observations reflect the stabilizing effect of (i) benzo-fusion, (ii) solvent and (iii) substitution on **3** or **4**. *o*-Cyclization of **3** \rightarrow **9** has a higher energy demand of ca. 1.5–2.5 kcal/mol than its **4** \rightarrow **10** counterpart. On the other hand, **9a–c** appears to be more stable than **10a–c** by ca. 1.5–3.0 kcal/mol and ca. 6.0 kcal/mol than the **10d** derivative. These variations may be attributed to a larger perturbation of the π density in **10**, induced by the 1,2-fusion of the isoxazole ring and its N–O dipole, onto the naphthalene core. The *o*-(1,5)-cyclization of **3** and **4** minima towards **9** and **10** in the presence of AcOH further

stabilizes the transition states up to 3.5 kcal/mol while that for the overall reaction to **9** and **10** up to 3 kcal/mol (Fig. 3).

The N–O₂ bond in **10** or **9** falls within the range 1.202–1.242 Å found in furoxans⁷⁴ and it remains as short as in the NO₂ group (Table 2), a feature common to heteroaromatic *N*-oxides.⁷⁵ The ring N–O₁ bond in **9** is quite stretched (ca. 1.492 Å) and compares with the most strained bonds in fused furoxans. This bond is slightly shorter in **10**. The corresponding N–O₁ bond length of their deoxygenated congeners is shorter by 0.07 Å (Table 2). Interestingly, the C₁–O₁ bond appears within a range of 1.348–1.368 Å, thus, implying some double bond character of this bond.

3.2. *peri*-Cyclization

peri-Cyclization (Scheme 1) to either **12** or **14** may take place through the O- (Scheme 1, path (v)) or N-site (Scheme 1, path (vi)) of the NO group, respectively. The latter may act as either an electrophile or a nucleophile. The first and key step in either path is the formation of the ring (**11** or **13** in Scheme 1).

3.2.1. 1,6-Cyclization. 1,6-Cyclization to **12** occurs through the E_1 conformer and may be envisaged to proceed by way of two alternative reaction paths (Scheme 1, **11**). Energy requirements for their minima and transition states are depicted in Fig. 4 (via path vii) and Fig. 5 (via path viii) and in Fig. 4S (via path vii) and Fig. 5S (via path viii).

Energy barriers (reflecting the distortion of the transition state geometry) for some intermediates are quite high, for example, **17** \rightarrow **12**, having an energy barrier in the range of 56.6–58.9 kcal/mol (Fig. 4S). Slightly lower energy demands, in the range of 1–2 kcal/mol, are observed in CH₂Cl₂ and THF compared with those in the gas phase. A marked drop for the energy barriers in the presence of AcOH is generally observed. For example, for the

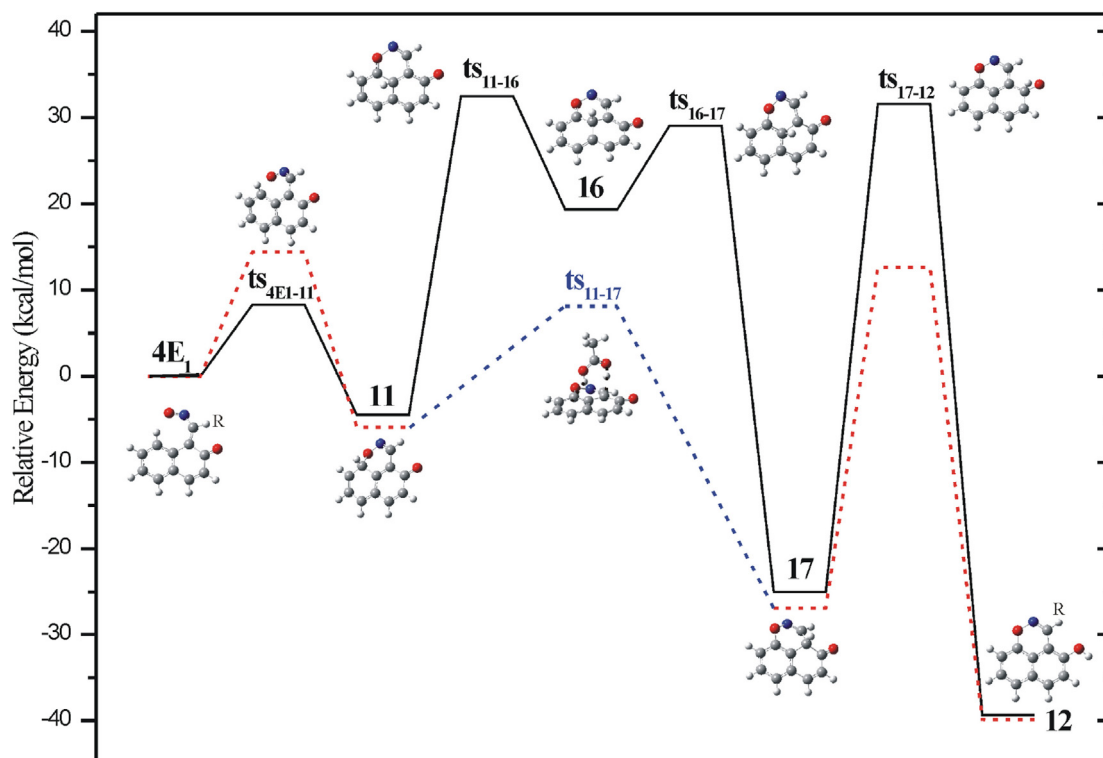
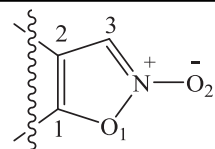
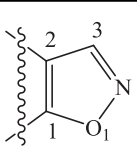


Fig. 4. Relative energies corrected for ZPE of the *peri*-(1,6)-cyclization (via path vii, Scheme 1) of **4** minimum to **12** (solid black line) and in the presence of AcOH (dashed lines) for R=H (C atoms=gray spheres, H=white, O=red and N=blue) (**ts**₁₁₋₁₇ only in AcOH).

Table 2
Bond lengths (Å)^a and angles (degrees)^a of the *N*-oxides **9** and **10** compared to their deoxygenated analogues

				
	Expt ^b	9	10	
N–O ₂		1.247	1.215	1.217
N–O ₁		1.468	1.492	1.485
C ₃ –N		1.319	1.323	1.325
C ₁ –O ₁		1.368	1.356	1.354
C ₁ –O ₁ –N		103.9	105.1	105.1
				1.416(1.412) ^c
				1.302(1.306)
				1.356(1.351)
				108.1(108.2)

^a B3LYP/6-311G+(d,p) level of theory.

^b Experimental values from X-ray analysis, Ref. 76.

^c Values refer to the deoxygenated derivatives of **9** and in parenthesis of **10**.

17→**12** conversion, the energy barrier is reduced by about 20 kcal/mol. The largest one, however, of ca. 39 kcal/mol is observed for the **23**→**12** conversion (Fig. 5). Apparently, AcOH facilitates an H transfer, taking place not only contiguously but also more interestingly through hopping⁷⁷ or tunnelling,⁷⁸ perhaps, as shown by the additional transition states corresponding to H transfer between non adjacent C positions (see Figs. 2, 4 and 5). This may well account for the 20 kcal/mol drop (Fig. 4) while the lower still energy demand of 39 kcal/mol transition (Fig. 5) may be regarded as the preferred one. It is to be noted that AcOH facilitates H transfers between C atoms, which are not adjacent. As a result, AcOH intervenes in the process (Fig. 4, path vii and Fig. 5, path viii). For instance, **11** is converted to **17** in two steps, via **16** (path vii), without AcOH while in the presence of AcOH, the same conversion can occur as a one-step process, via the **ts**₁₁₋₁₇

transition state with an overall activation energy drop of 23 kcal/mol.

3.2.2. 1,5-Cyclization. 1,5-Cyclization occurs through the *E*₂ conformer (Scheme 1, path (vi)). Energy demands for minima and transition state structures are given in Fig. 6 and Fig. 6S. The formation of the final quinonoid structure **14** may be explained on the same grounds as in **12**. This is in evidence by the notably lower energy barrier to cyclization of **4b–d**, in the range of ca. 5.1–6.3 kcal/mol compared with that of its parent structure **4a** of ca. 15 kcal/mol, in the gas phase. The inherent ring strain in **15**, a result of accumulated π-density (see earlier arguments on **9** and **10**), discourages its formation, in favour of **14**. It is of interest to note that substitution, once again, confers stability on **14**. The reaction (total) energy for the conversion **4E**₂→**14** is 26.8, 32.7, 33.4 and 35.6 kcal/mol for the **a–c** derivatives in the gas phase. A lower energy demand of 1–3 kcal/mol is observed in CH₂Cl₂ and THF. Again, the presence of AcOH results in a significant decrease of the energy demand by about 30 kcal/mol (see Fig. 6). As shown in Fig. 6, in the absence of AcOH, **13** is converted to **14** via **24**, in a two-step process while the presence of AcOH, effects the same conversion in one-step, via the **ts**₁₃₋₁₄ transition state, with an overall activation energy drop from 35 to 5 kcal/mol.

It should be noted that the diagrams for the relative energies, relative enthalpies and free Gibbs energies for the *o*-(1,5)-, *peri*-(1,6)- and (1,5)-cyclizations of **3** or **4** minima to **9**, **10**, **12** or **14** are similar to the relative energies corrected for ZPE depicted in Figs. 3–6.

3.3. Reflections on the cyclization profile of **3** and **4**

Experimental findings on the cyclization of **3** or **4**, oxidatively generated from the oximes **5** or **6**, have been quite intriguing, with regard to the varying reaction outcomes.^{43–45} Accordingly, **3b,c** and

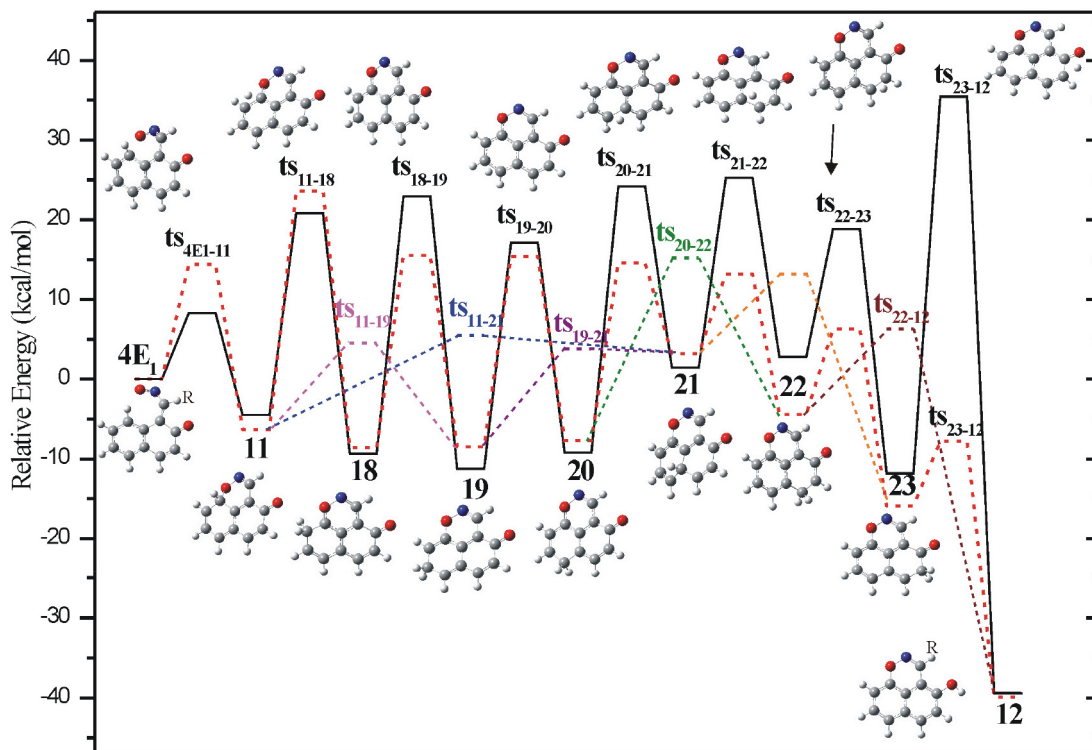


Fig. 5. Relative energies corrected for ZPE of the *peri*-(1,6)-cyclization (via path viii, Scheme 1) of **4** minimum to **12** (solid black line), in the presence of AcOH (dashed lines) for R=H (C atoms=gray spheres, H=white, O=red and N=blue).

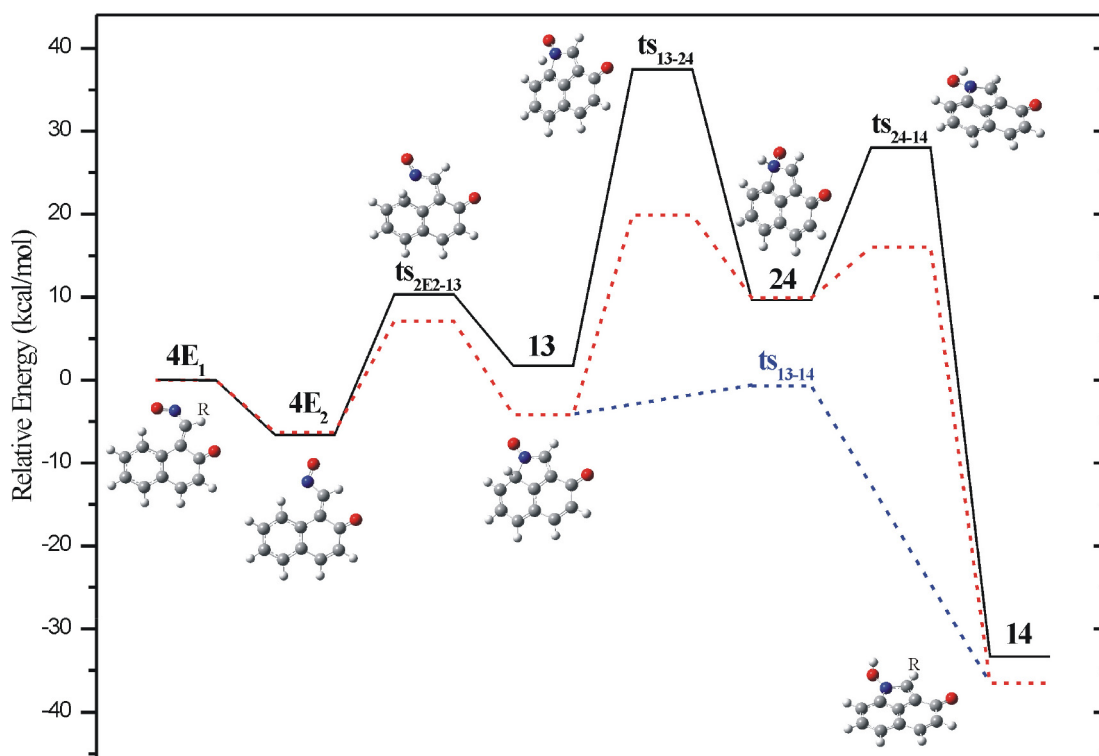


Fig. 6. Relative energies corrected for ZPE of the *peri*-(1,5)-cyclization of **4** minimum to **14** (solid black line) and in the presence of AcOH (dashed lines) for R=H (C atoms=gray spheres, H=white, O=red and N=blue).

4a–d give the corresponding **9** and **10**, respectively (Scheme 1, path (iv)) while **3a** is quite temperamental, furnishing mainly hydrolysis and polymerization products.^{42,43} The latter is a hardly surprising result, taking note of (a) the propensity of **3a** to rapid re-

aromatization and (b) the C-3 unsubstituted reactive position of **9**, as soon as it is formed, giving rise to other, alternative to cyclization, competing reactions. An analogous primary *o*-cyclization is shown by **4a**. In that case, however, benzo-fusion (a) confers

stabilization and (b) offers alternative *peri*-cyclization routes (Scheme 1, paths (v) and (vi)).^{43,44,46}

Lead (IV) acetate (LTA) oxidation of oximes **5** or **6** produces both **12** and **14**⁷⁸ while the use of phenyliododiacetate (PIDA) as oxidant, under similar conditions, directs the reaction selectively to **12**.^{43–45,79} Worth noting is that the reaction proceeds equally well in solvents of varying polarity, for example, THF, CH₂Cl₂ mainly but also in MeCN.

This oxidant-selective outcome may be correlated to the O–X bond dissociation enthalpy in the transient complexes **7** or **8** (Scheme 1).⁸⁰ The easier the O–X rupture, the faster will be the cyclization of the resulting intermediates **3** or **4** to the corresponding *N*-oxides **9**, **10** or 1,2-oxazine **12**. Indeed, bond dissociation enthalpies of ca. 91.17 and ca. 55.60 kcal/mol have been reported for Pb–O and I–O in various compounds.⁸⁰ The notably stronger former bond, of an estimated length of ca. 2.25–2.30 Å, probably attributed to a multiple back-bonding from Pb lone pairs⁸¹ is apparently the toughest to cleave. Accordingly, of the corresponding complexes **7** or **8**, the Pb-based ones have the highest energy demands for cyclization. An energy demanding six-membered pseudo chelate ring structure for these complexes may also be regarded as a viable possibility. The experimental outcomes are, indeed, consistent with these arguments.

Both oxidants release acetic acid during the reaction, regardless of the solvent used, unless it is trapped. Thus, the overall process is, in effect, dominantly acid-catalyzed by way of a 1,5-electrocyclization of **3** or **4** to **9** or **10**^{43,44} or a 1,6 (5)-electrocyclization and sequential H shifts to **14** and/or **12**⁸² (Scheme 1). The latter may be effected by hydrogen scrambling (a) *intramolecularly*, via a trajectory of successive shifts or (b) *intermolecularly*, via either acid- or solvent-assisted proton shuttling.^{83,84} It is the trajectory mode of the successive H shifts that differentiates between the two paths.

H transfer (polar or radical in nature), an arguably important process in chemistry and biology, is usually fast but it can become rate determining if catalyzed. This is especially true when the transfer is to and from C atoms or concerted bond cleavage and formation among heavy atoms (i.e., non H atoms).

H transfer, in our case, does not necessarily impart a kinetic advantage towards stabilizing the transition states, it rather complements the thermodynamic driving force, through re-aromatization, to the end-products. The latter, perhaps, may side-step the formation of charged intermediates.

Given that the activation energy is inversely related to the solvent dielectric constant,⁸⁵ the insignificant drop of the activation barriers, in the range of 1–3 kcal/mol, in other solvents, may be indicative of a rather negligible sensitivity of the reaction path to solvent polarity. Yet, this observation cannot still firmly point to the identity of the engaged species (be that dipolar, diradical or neutral).

HOMA, I_A and ABO/BOD indices have been chosen as the most responsive to the observed outcomes. Calculated HOMA values (Table 3) are consistent with a massive revert-to-type process to the extent of 81–95%. Comparing, however, the overall aromaticity change in the reaction sequences (Scheme 1), a substantial decrease is evident in the fused heterocycles **9**, **10**, **12** and **14**. A drop in the range of 23–51% is estimated in going from the oximes **5** and **6** to **9**, **10**, **12** or **14**. Certain features are of particular interest (a) the generation of *o*-quinone methide intermediates **3** and **4** is accompanied by a rise of 23% and 7%, respectively, followed by a ca. 28% drop towards the products, (b) the reaction coordinate encompasses successive transition states,⁸⁶ activation barriers being due to their geometry distortion, (c) the aromatic character of **9** and **10** compares well with that of **12**, (d) **10** shows a markedly lower aromatic character against **15**. (e) *peri* (1,8)- fusion appears to increase the diene geometry of the tricycles **12** and **14**, (f)

a naphthalene-based *peri*-fused tricycle **12** appears to have an aromatic character of comparable magnitude to a quinonoid tricycle, like **14**, of distinct diene geometry, (g) **15**, with a higher aromatic ‘arrangement’ than the rest, cannot survive due to the severe strain inherent in the five-membered *peri* (1,8)-fused ring exacerbated by the N–O dipole-induced accumulated ring π -density.

Table 3

Calculated rHOMA, I_A and ABO/BOD values for heterocycles **9**, **10**, **12**, **14**, **15** and their precursors *o*-quinone methides **3**, **4** and oximes **5**, **6** (a: R=H)^a

	rHOMA			I_A	ABO/BOD
	Z	E_1	E_2		
3	0.971 ^b	^c			
4	0.818 ^b	0.026	0.101		
5	0.787 ^b	0.923	0.951		
6	0.764 ^b		0.778		
9		0.476 ^d		90.20 ^d	1.607/0.229 ^d
10		0.550 ^d			1.638/0.163 ^d
12		0.585		109.10	1.296/0.077
14		0.528		112.43	1.281/0.078
15		0.740		164.25	1.306/0.042

^a B3LYP/6-311G+(d,p).

^b Ref. 46.

^c Insignificantly low value.

^d Ref. 82.

Compounds **3** and **4**, in their *Z* conformation, show higher HOMA values than their precursor oximes **5** and **6**, respectively (Table 3). Geometry optimization has demonstrated the development of an extended π delocalization into a five-membered *N*-oxide ring, through *o*-(1,5)-cyclization.⁴⁶ The end-products *N*-oxides **9** and **10**, on the other hand, indicate markedly lower HOMA values. The extent of delocalization, gradually building up along the reaction path, reaching the successive transition states, subsequently descends towards the end product. It is the N–O dipole, in the latter that has been incriminated for this change.⁸⁷ The issues of stabilization through resonance or extended conjugation are in effect, herein. Indeed, **12** and **14** have HOMA values of comparable magnitude (Table 3). Apparently both have an inherent extended diene character, as their common stabilizing factor, of different origin, nonetheless, that is, localized π frames due to *peri*-fusion in **12**, and benzo-fused quinone type in **14**.

Bond uniformity I_A and bond order ABO/BOD variations (Table 3) follow, in general, the HOMA portrait. Accordingly, the aromatic character increases in going from the *N*-oxides **9** and **10** to the *peri*-fused **12**, **14** and the fictitious **15**, in concert with a corresponding increase of their diene character. The only discordance is the reverse order of magnitude among the HOMA and I_A of **12** and **14**.

In as much as aromaticity reflects stability one expects that the former lags behind bonding changes at the transition states (in other words, its loss or drop should be ahead of these changes) leading to an increase of ΔG^\ddagger along the reaction path. Interestingly, a benzo-fused quinone stabilization in **14** (an optimal orbital alignment, perhaps?) could be similarly accounted for a comparable ΔG^\ddagger increase in the corresponding reaction path. In both cases, aromaticity changes of transition structures, as the reaction progresses, are confirmed from the bond length changes of the quinone and the nitrosoalkene entities (Tables 4S–7S).

Substitution also introduces selectivity in the reaction outcome (Tables 4 and 5). What is more interesting is that substitution follows the pattern observed for oxidant selectivity. Indeed, oxidation of oximes **6b–d** with PIDA leads selectively to **12d** or **10b**, c, i.e., alkyl substitution favours *o*-cyclization whereas aryl substitution prefers exclusively *peri*-(1,6)-cyclization. Oxidation with LTA, on the other hand, appears to be substituent-insensitive and leads to both **12** and **10** in a 3:2 ratio.

Table 4
Reaction energies^a (kcal/mol) for *o*- and *peri*-cyclization structures of **4** to **10**, **12** and **14**^b

Reaction	H	H ^c	Me	Et	Ph
4E ₁ → 10	-14.0(-13.9)[-13.9]	-17.2(-17.0)[-17.0]	-18.1(-18.6)[-18.7]	-18.1(-18.6)[-18.7]	-17.3(-17.1)[-17.0]
4E ₁ → 12	-39.4(-40.1)[-40.1]	-39.9(-40.2)[-40.3]	-41.1(-42.1)[-42.2]	-40.5(-41.6)[-41.7]	-38.2(-39.4)[-39.4]
4E ₁ → 14	-33.3(-35.4)[-35.5]	-36.5(-38.4)[-38.5]	-39.2(-42.2)[-42.3]	-39.1(-42.1)[-42.3]	-39.1(-40.9)[-40.9]
4E ₂ → 14	-26.8(-28.4)[-28.5]	-30.2(-32.1)[-32.2]	-32.7(-35.1)[-35.2]	-33.4(-35.8)[-35.9]	-35.6(-36.4)[-36.4]

^a At the B3LYP/6-311G+(d,p) level of theory; data in the gas phase (in THF solvent) [in CH₂Cl₂ solvent].^b a: R=H, b: R=Me, c: R=Et, d: R=Ph.^c Structures interacting with AcOH.**Table 5**
Reaction zero point energies corrected ΔE_0 (kcal/mol), enthalpies ΔH (kcal/mol) and free energies ΔG (kcal/mol) for *o*- and *peri*-cyclization structures of **3** to **9**, and **4** to **10**, **12** and **14**^a

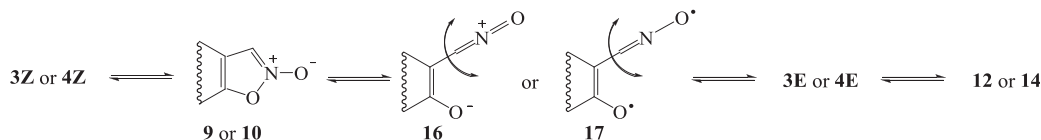
Reaction	H			H ^b			Me			Et			Ph		
	ΔE_0	ΔH	ΔG	ΔE_0	ΔH	ΔG	ΔE_0	ΔH	ΔG	ΔE_0	ΔH	ΔG	ΔE_0	ΔH	ΔG
3E ₁ → 9	14.8	15.6	13.4	17.6	18.3	16.5	18.3	19.4	16.6	19.1	19.8	18.2	20.8	21.7	19.0
4E ₁ → 10	12.6	13.3	11.3	15.8	16.4	14.6	16.5	17.1	15.5	16.4	17.0	15.2	15.4	16.1	14.4
4E ₁ → 12	38.1	38.6	36.9	38.4	39.1	37.1	39.6	40.0	38.6	38.8	39.4	37.6	36.6	37.1	35.7
4E ₁ → 14	31.8	32.2	30.8	34.8	35.4	33.5	37.5	37.7	36.7	37.4	37.7	36.8	37.2	37.5	36.2

^a At the B3LYP/6-311G+(d,p) level of theory; data in the gas phase; a R=H, b R=Me, c R=Et, d R=Ph.^b Structures interacting with AcOH.

It is, therefore, clear that 1,6-cyclization competes with its 1,5-rivals, in terms of geometry and energy constraints of the process. Relative energies of both *o*- and *peri*-cyclization modes suggest that **12** and **14** have comparable stabilities (Tables 4 and 5), indicating a stability order **12** ≥ **14** > **9** > **10**. We observe an overall stabilization of the reaction, up to 3 kcal/mol, in AcOH (see Tables 4 and 5) while this catalyst has a marked stabilizing effect on the minima or transition states (Fig. 5, **ts**₂₃₋₁₂ or Fig. 6, **ts**₂₄₋₁₄) (see also Sections 3.2.1 and 3.2.2 earlier).

From the data at hand and their analysis the following question is inevitably raised: 'is *peri*-annulation to **12** or **14** a primary or a secondary process?' That is, does **4** assume the *E* conformation directly, as soon as it is generated (primary process) or does it do it through its *Z* variant, *o*-cyclization to **10**, re-opening of the latter and isomerization (secondary process)? A primary process should require that the precursor oxime (Scheme 1) takes up its *E*-conformation, followed by its oxidation through the complex **7** or **8** and its eventual collapse directly to **4E** (*E*₁ or *E*₂). The *Z*-conformation of oxime **6a** is more stable than its *E*-variant by 7.7 kcal/mol. The energy cost for their *E*-to *Z*-conversion is 4.2 kcal/mol. In a secondary process, on the other hand, the required *Z* → *E* conversion should go through the intermediacy of a form of **4**.⁴⁶

Indeed, **4** cyclizes to **10** readily, via its *Z* conformer, with a very low or no energy barrier and this has been experimentally observed.⁴³ Unsubstituted **10** (i.e., **10a**) re-opens equally readily and assumes the *E* conformation⁸⁸ (Scheme 2), ultimately cyclizing to **12** or **14**.

**Scheme 2.** Isomerization rearrangement of β -nitroso-*o*-quinone methides **3** and **4**.

The N–O₁ bond compressed among accumulated π -density of a distorted ring^{46,74} is seriously weakened⁸⁶ and suffers facile rupture, when triggered. It is the lability of H-3 in **9** or **10** that provides that trigger. The isoxazole ring, once opened, may revert to its *Z* precursor or change into its *E* counterpart (Scheme

2), eventually undergoing a *peri*-cyclisation. Thus, it is reasonable to assume an equilibrium among the proposed *o*-quinone methide forms⁴⁶ prior to final cyclization. It is worth noting that the *Z* → *E* conversion can be envisaged through a dipolar (zwitterionic) species, such as **16** (Scheme 2). A biradical species, such as **17** (Scheme 2), on the other hand, would be consistent with some of the calculated high energy barriers (Figs. 3–6). However, the comparable barrier magnitudes calculated in solution (see earlier comments), cannot safely favour one of the possible arrangements of the intermediate species. The estimated rise in HOMA values (Table 3), during the generation of **3** and **4**, lends support to an 'aromatic' arrangement like **16** without ruling out that of **17**.

The energy barriers of these successive changes range from 12 to 16 kcal/mol, 16–32 kcal/mol and 6–9 kcal/mol, respectively. These energy costs can be supplied by the total reaction energy of ca. 38–42 kcal/mol for the most favoured reaction **4E**₁ → **12**.

The reaction **4a** → **12** is favoured over its competitor **4a** → **14** by ca. 6 kcal/mol (i.e., the former has a higher total reaction energy of 39.3(40.1) kcal/mol over the latter of 33.3(35.4) kcal/mol, in the gas phase (or in solution)). Interestingly, the reactions **4b–d** → **12** and **4b–d** → **14** of the other derivatives have comparable reaction energies. However, the largest barrier in the sequence of the most favoured route of **4** → **12** exceeds that of **4** → **14** by ~10 kcal/mol. This indicates a larger distortion of the relevant transition state and is consistent with the observed much longer time taken for the cyclization reaction to be completed.⁸⁸

Overall, it appears that the 1,6-sequence is the preferred *peri*-cyclization mode. However, it is of interest that whether this is the prevalent or the sole reaction path will depend primarily on the oxidant-directed conformation and subsequent collapse of **7** or **8** and not that of *o*-quinone methides **3** or **4**. The reaction is so fast

that takes precedence over any other that could compete through the presence of a nucleophile.⁴⁴ The term ‘reclusive’ is, therefore, coined to identify its uniqueness.

4. Conclusions

The intramolecular cyclization of **3** and **4** is a reclusive process in that it takes precedence over any other from external stimuli. It follows an oxidant-dependent 1,6- or a competing 1,5-electrocyclization. This selectivity appears to be correlated to the dissociation enthalpy of the O–Pb or I–O bond of the Pb- or I-based intermediate complexes **7** or **8**.

Regardless of the solvent used, it appears that the dominant reaction medium, unless trapped, is AcOH, liberated by both oxidants. Intramolecular or intermolecular solvent-assisted, contiguous or not, H shift trajectories, probably through hopping or tunnelling, account for the successive transition states involved and the substantial drop of activation barriers. Rather insignificant changes have been observed in other solvents, in the absence of AcOH, compared to those in the gas phase though stabilization, in all cases, was larger in solution. Thus, the proposed reaction paths, apparently, do not favour charged species.

Substitution follows the oxidant selectivity pattern. Accordingly, in PIDA, alkyl substitution prefers the *o*-(1,5)-cyclization to *N*-oxides **9** or **10** and aryl substitution favours the *peri*-(1,6)-cyclization to 1,2-oxazine **12**. LTA, on the other hand, proves to be substituent-insensitive, giving rise to all cyclization products.

Aromaticity indices, as stability indicators of the end structures, cannot discriminate between competing paths, as their values are of comparable magnitude. They do, however, suggest a markedly lower aromaticity of the heterocycles compared to their precursors, attributed to the *peri*-triggered enhanced diene geometry of their π -frame.

The available evidence cannot irrefutably clarify whether the *peri*-cyclization is a primary or a secondary process. It appears that the preferred path is oxidant-directed.

The reaction takes precedence over any other that could compete through the presence of a nucleophile and has been termed ‘reclusive’ to identify its uniqueness.

Supplementary data

Supplementary data related to this article can be found at <http://dx.doi.org/10.1016/j.tet.2014.11.020>.

References and notes

- Van de Water, R. W.; Pettus, T. R. *Tetrahedron* **2002**, *58*, 5367.
- Pathek, T. P.; Singman, M. S. *J. Org. Chem.* **2011**, *76*, 9210.
- Chen, M. W.; Cao, L. L.; Ye, Z. S.; Jiang, G. F.; Zhou, Y. G. *Chem. Commun.* **2013**, 1660.
- Willis, N. J.; Bray, C. D. *Chem.—Eur. J.* **2012**, *18*, 9160.
- Wang, H.; Wahl, M. S.; Rokita, S. E. *Angew. Chem., Int. Ed.* **2008**, *47*, 1291.
- Sharma, A.; Santos, I. O.; Gaur, P.; Ferreira, V. E.; Garcia, C. R. S.; da Rocha, D. R. *Eur. J. Med. Chem.* **2013**, *59*, 48.
- Han, I.; Russell, D. J.; Kohn, H. J. *Org. Chem.* **1992**, *57*, 1799.
- Tomasz, M.; Das, A.; Tang, K. S.; Ford, M. G. J.; Minnock, A.; Musser, S. M.; Waring, M. J. *J. Am. Chem. Soc.* **1992**, *114*, 11581.
- Angle, S. R.; Rainier, J. D.; Woytowicz, C. J. *Org. Chem.* **1997**, *62*, 5884.
- Angle, S. R.; Yang, W. J. *J. Org. Chem.* **1992**, *57*, 1092.
- Gaudiano, G.; Frigerio, M.; Bravo, P.; Koch, T. H. *J. Am. Chem. Soc.* **1990**, *112*, 6704.
- Amouri, H.; Le Bras, J. *Acc. Chem. Res.* **2002**, *35*, 501.
- Chiang, Y.; Kresge, A. J.; Zhu, Y. *J. Am. Chem. Soc.* **2000**, *122*, 9854.
- Shaikh, A. K.; Cobb, A. J. A.; Varvounis, G. *Org. Lett.* **2012**, *14*, 584.
- Freccero, M. *Mini-Rev. Org. Chem.* **2004**, *1*, 403.
- Di Valentini, C.; Freccero, M.; Zanaletti, R.; Sarzi-Amade, M. *J. Am. Chem. Soc.* **2001**, *123*, 8366.
- Weinert, E. E.; Dondi, R.; Colloredo-Melz, S.; Frankenfield, K. N.; Mitchell, C. H.; Freccero, M.; Rokita, C. E. *J. Am. Chem. Soc.* **2006**, *128*, 11940.
- Sugimoto, H.; Nakamura, S.; Ohwada, T. *Adv. Synth. Catal.* **2007**, *349*, 669.
- Barrero, A. F.; Quilez del Moral, J. F.; Mar Herrador, M.; Arteaga, P.; Cortes, M.; Benites, J.; Rosellon, A. *Tetrahedron* **2006**, *62*, 6012.
- Dell, C. P. *J. Chem. Soc., Perkin Trans. 1* **1998**, 3873 and references cited therein.
- Tietze, L.; Ketschau, G. *Top. Curr. Chem.* **1997**, Metz, P., Eds.; Springer: Berlin, Heidelberg, Germany, pp 1–120.
- Wan, P.; Barker, B.; Diana, L.; Fischer, M.; Shi, Y.; Yang, C. *Can. J. Chem.* **1996**, *74*, 465.
- Basarić, N.; Doslic, N.; Ivković, J.; Wang, Y. H.; Malis, M.; Wan, P. *Chem.—Eur. J.* **2012**, *18*, 10617.
- Bentley, T. W. *Org. Biomol. Chem.* **2011**, *9*, 6685.
- Chiang, Y.; Kresge, A. J.; Zhu, Y. *J. Am. Chem. Soc.* **2001**, *123*, 8089.
- Chiang, Y.; Kresge, A. J.; Zhu, Y. *J. Am. Chem. Soc.* **2002**, *124*, 717.
- Modica, E.; Zanaletti, R.; Freccero, M.; Mella, M. *J. Org. Chem.* **2001**, *66*, 41.
- Tsoungas, P. G. *Heterocycles* **2002**, *57*, 915 and references cited therein.
- Tsoungas, P. G. *Heterocycles* **2002**, *57*, 1149 and references cited therein.
- Marwaha, A.; Singh, P.; Mahajan, M. P. *Tetrahedron* **2006**, *62*, 5474 and references cited therein.
- Yang, B. Y.; Zollner, T.; Gebhardt, P.; Mollmann, U.; Müller, M. *J. Org. Biomol. Chem.* **2010**, *8*, 691.
- Bodnar, B. S.; Miller, M. J. *Angew. Chem., Int. Ed.* **2011**, *50*, 5629.
- Wieser, K.; Berndt, A. *Angew. Chem., Int. Ed. Engl.* **1975**, *14*, 70.
- Francotte, E.; Merenyi, R.; Vandebulcke-Coyette, B.; Viehe, H. G. *Helv. Chim. Acta* **1981**, *64*, 1208.
- Smith, J. H.; Heidema, J. H.; Kaiser, E. T. *J. Am. Chem. Soc.* **1972**, *94*, 9276.
- Veronese, A. C.; Vecchiati, G.; Sferra, S.; Orlandini, P. *Synthesis* **1985**, 300.
- Kwiatkowski, M.; Kwiatkowski, E.; Olechnowicz, A.; Ho, D. M.; Deutsch, E. *J. Chem. Soc., Dalton Trans.* **1990**, 2497.
- Davies, D. E.; Gilchrist, T. L.; Roberts, T. G. *J. Chem. Soc., Perkin Trans. 1* **1983**, 1275.
- Gilchrist, T. L.; Roberts, T. G. *J. Chem. Soc., Perkin Trans. 1* **1983**, 1283.
- Zimmer, R.; Reissig, H. U. *J. Org. Chem.* **1992**, *57*, 339.
- Reissig, H. U.; Hippeli, C.; Arnold, T. *Chem. Ber.* **1990**, *123*, 2403.
- Boulton, A. J.; Tsoungas, P. G.; Tsiamis, C. J. *Chem. Soc., Perkin Trans. 1* **1986**, 1665.
- Supsana, P.; Tsoungas, P. G.; Aubry, A.; Skoulika, S.; Varvounis, G. *Tetrahedron* **2001**, *57*, 3445.
- Dolka, C.; Van Hecke, K.; Van Meervelt, L.; Tsoungas, P. G.; Van der Eycken, E. V.; Varvounis, G. *Org. Lett.* **2009**, *11*, 2964.
- Liaskopoulos, T.; Skoulika, S.; Tsoungas, P. G.; Varvounis, G. unpublished work.
- Kozielewicz, P.; Tsoungas, P. G.; Tzeli, D.; Petsalakis, I. D.; Zloh, M. *Struct. Chem.* **2014**, *25*, 1711.
- Smith, J. A.; Le, Q.; Jones, E. D.; Deadman, J. *Future Med. Chem.* **2010**, *2*, 215.
- Ikeda, R.; Kuwano, R. *Molecules* **2012**, *17*, 6901.
- Searcey, M.; Grewal, S. S.; Madeo, F.; Tsoungas, P. G. *Tetrahedron Lett.* **2003**, *44*, 6745.
- Becke, A. D. *J. Chem. Phys.* **1993**, *98*, 1372.
- Lee, C.; Yang, W.; Parr, R. G. *Phys. Rev. B* **1988**, *37*, 785.
- Curtiss, L. A.; McGrath, M. P.; Blandeau, J.-P.; Davis, N. E.; Binning, R. C., Jr.; Radom, L. *J. Chem. Phys.* **1995**, *103*, 6104.
- Zhang, J.-P.; Zhou, X.; Bai, F. Q.; Zhang, H. X.; Tang, A. C. *Theor. Chem. Acc.* **2009**, *122*, 31.
- Wang, H.; Meng, F. *Theor. Chem. Acc.* **2010**, *127*, 561.
- Irfan, A.; Zhang, J.-P.; Chang, Y. F. *Theor. Chem. Acc.* **2010**, *127*, 587.
- Tzeli, D.; Petsalakis, I. D.; Theodorakopoulos, G. *Phys. Chem. Chem. Phys.* **2011**, *13*, 954.
- Simón, L.; Goodman, J. M. *Org. Biomol. Chem.* **2011**, *9*, 689.
- Dunning, T. H., Jr. *J. Chem. Phys.* **1989**, *90*, 1007 Woon, D.; Dunning, T. H., Jr. *J. Chem. Phys.* **1995**, *103*, 4572.
- Zhao, Y.; Truhlar, D. *Theor. Chem. Acc.* **2008**, *120*, 215.
- Tomasi, J.; Mennucci, B.; Cammi, R. *Chem. Rev.* **2005**, *105*, 2999 Pedone, A.; Bloino, J.; Monti, S.; Prampolini, G.; Barone, V. *Phys. Chem. Chem. Phys.* **2010**, *12*, 1000.
- Boys, S. F.; Bernardi, F. *Mol. Phys.* **1970**, *19*, 553 Xantheas, S. S. *J. Chem. Phys.* **1994**, *104*, 8821.
- Frisch, M. J.; Trucks, G. W.; Schlegel, H. B.; Scuseria, G. E.; Robb, M. A.; Cheeseman, J. R.; Scalmani, G.; Barone, V.; Mennucci, B.; Petersson, G. A.; Nakatsuji, H.; Caricato, M.; Li, X.; Hratchian, H. P.; Izmaylov, A. F.; Bloino, J.; Zheng, G.; Sonnenberg, J. L.; Hada, M.; Ehara, M.; Toyota, K.; Fukuda, R.; Hasegawa, J.; Ishida, M.; Nakajima, T.; Honda, Y.; Kitao, O.; Nakai, H.; Vreven, T.; Montgomery, J. A., Jr.; Peralta, J. E.; Ogliaro, F.; Bearpark, M.; Heyd, J. J.; Brothers, E.; Kudin, K. N.; Staroverov, V. N.; Kobayashi, R.; Normand, J.; Raghavachari, K.; Rendell, A.; Burant, J. C.; Iyengar, S. S.; Tomasi, J.; Cossi, M.; Rega, N.; Millam, J. M.; Klene, M.; Knox, J. E.; Cross, J. B.; Bakken, V.; Adamo, C.; Jaramillo, J.; Gomperts, R.; Stratmann, R. E.; Zayzev, O.; Austin, A. J.; Cammi, R.; Pomelli, C.; Ochterski, J. W.; Martin, R. L.; Morokuma, K.; Zakrzewski, V. G.; Voth, G. A.; Salvador, P.; Dannenberg, J. J.; Dapprich, S.; Daniels, A. D.; Farkas, O.; Foresman, J. B.; Ortiz, J. V.; Cioslowski, J.; Fox, D. J. *Gaussian 09, Revision A.1*; Gaussian: Wallingford, CT, 2009.
- Poater, J.; Duran, M.; Sola, M.; Silvi, B. *Chem. Rev.* **2005**, *105*, 3911.
- Raczyńska, E. D.; Hallman, M.; Kolczyńska, K.; Stępniewski, T. M. *Symmetry* **2010**, *2*, 1485.
- Frizzo-Marcos, C. P.; Martins, A. P. *Struct. Chem.* **2012**, *23*, 375.
- Bird, C. W. *Tetrahedron* **1997**, *53*, 3319.
- Bird, C. W. *Tetrahedron* **1996**, *52*, 9945.
- Mattito, E.; Salvador, P.; Duran, M.; Solà, M. J. *Phys. Chem.* **2006**, *110*, 5108.
- Jursic, B. S. *Tetrahedron* **1997**, *53*, 13285.
- Rauhut, G. *J. Org. Chem.* **2001**, *66*, 5444 and references cited therein.

71. Davies, I. W.; Guner, V. A.; Houk, K. N. *Org. Lett.* **2004**, *6*, 743 and references cited therein.
72. Pilepic, V.; Ursic, S. J. *Mol. Struct. THEOCHEM* **2001**, *538*, 41 and references cited therein.
73. Leach, A. G.; Houk, K. N. *Org. Biomol. Chem.* **2003**, *1*, 1389.
74. Pasinszki, T.; Havasi, B.; Hajgato, B.; Westwood, N. P. C. *J. Phys. Chem. A* **2009**, *113*, 170.
75. Sivasubramanian, G.; Parameswaran, V. R. J. *Heterocycl. Chem.* **2007**, *44*, 1223 and references cited therein.
76. Chiari, G.; Viterbo, D. *Acta Crystallogr. B* **1982**, *38*, 323.
77. Voth, G. A. *Acc. Chem. Res.* **2006**, *39*, 143 and references cited therein.
78. Marx, D.; Tuckerman, M. E.; Hutter, J.; Parrinello, M. *Nature* **1999**, *397*, 601.
79. Lead(IV)acetate oxidation of **4** gives **12** and **14** in moderate yields and a spiro dimer as the major product (see Ref. 43). Phenyliododiacetate (PIDA) oxidation, furnishes **12** selectively (see Ref. 47). On the other hand, the oxidation can be selectively driven to the dimer, if run in AcOH/TFA or to **12** (as with PIDA) in the presence of N-morpholine oxide (NMO) (see: Rosenau, T.; Mereiter, K.; Jäger, C.; Schmidt, P.; Kosma, P. *Tetrahedron* **2004**, *60*, 5719) and Ref. 43. Same reaction outcome is obtained with Ag₂O oxidant.
80. Luo, Y.-R. In *Handbook of Bond Dissociation Energies in Organic Compounds*; CRC LLC: Boca Raton, FL, 2003.
81. Siidra, O. I.; Krivovichev, S. V.; Filatov, S. K. Z. *Kristallogr.* **2008**, *223*, 114.
82. Balaban, A. T. *Chem. Rev.* **2004**, *104*, 2777.
83. Many experimental and theoretical reports, as well as book chapters and reviews, have been devoted to Proton Transfer (PT) phenomena. Tunneling (a quantum effect of going *through* and not *over* an energy reaction barrier) (see Ref. 76) or hopping (or 'hop-turn' or Grötthuss mechanism) are the currently accepted proton relay modes (see also: Alkorta, I.; Elguero, J. *Org. Biomol. Chem.* **2006**, *4*, 3096 and references cited therein).
84. Proton relay is a concept of growing interest and importance in deciphering mechanisms of many processes see: Bonin, J.; Costentin, C.; Robert, M.; Savaent, J.-M.; Tard, C. *Acc. Chem. Res.* **2012**, *45*, 372 and references cited therein.
85. Wang, H.; Wang, Y.; Han, K.-L.; Peng, X.-J. *J. Org. Chem.* **2005**, *70*, 4910 and references cited therein.
86. (a) von Ragué Schleyer, P.; Wu, J. I.; Cossio, F. P.; Fernandez, I. *Chem. Soc. Rev.* **2014**, *43*, 4909; (b) Birney, D. M. *Curr. Org. Chem.* **2010**, *14*, 1658.
87. Kozielowicz, P.; Tzeli, D.; Tsoungas, P. G.; Zloh, M. *Struct. Chem.* <http://dx.doi.org/10.1007/S11224-014-0459-6>.
88. (a) Unsubstituted **9** or **10** are not isolable, see also Ref. 79. (b) Aryl substituted **10**, upon prolonged reaction, leads to **12** whereas its alkyl substituted analogues give **14**: Supsana, P.; Tsoungas, P. G.; Tzeli, D.; Varvounis, G. unpublished work.